Backscattering of Ground Terrain and Building Materials at Millimeter-Wave and Terahertz Frequencies

D. A. DiGiovanni[a], A. J. Gatesman[a], R. H. Giles[a], and W. E. Nixon[b]
[a]Submillimeter-Wave Technology Laboratory, University of Massachusetts Lowell, Lowell, MA 01854
[b]United States Army National Ground Intelligence Center, Charlottesville, VA 22911

ABSTRACT

As terrestrial remote sensing and communication systems continue to evolve in the 0.1 – 0.3 THz band, the need to understand the scattering behavior of common materials and ground terrain at these frequencies becomes important. Terrain features and surface roughness that would otherwise appear smooth at longer wavelengths begin to significantly impact the radar cross section of the surfaces at these higher frequencies. The HH and VV polarized backscattering coefficient of several types of ground terrain and building materials were measured in indoor compact radar ranges operating at 100 GHz and 240 GHz. Measurements of the various materials were collected at elevation angles ranging from 5 to 35 degrees. The goal of the effort was to develop a better understanding of the polarimetric scattering behavior of materials in the 0.1 – 0.3 THz region.

Keywords: rough surface, scattering, ground terrain, building materials, terahertz, clutter

1. INTRODUCTION

The interest in electromagnetic scattering from common materials and ground terrain continues to increase as the number of systems developed for the 0.1 – 0.3 THz region continues to grow. Much work has been done on studying the dielectric and scattering properties of various types of terrain at microwave frequencies but relatively little work has been done at higher frequencies. The THz compact radar ranges at the Submillimeter-Wave Technology Laboratory (STL) were used in this work and provide a convenient means to study the backscattering behavior of objects at these frequencies. A preliminary investigation was made of the 100 GHz and 240 GHz radar backscattering coefficient of sand, gravel, topsoil with various moisture content, roofing shingles, and brushed and unbrushed concrete. The backscattering behavior of each terrain type was measured as a function of azimuth angle at a number of fixed elevation angles from 5 to 35 degrees.

1.1 Measurement Systems

The radar cross section (RCS) of the rough surfaces was measured in two fully polarimetric compact radar ranges. One of the ranges operated at 240 GHz and is described in [1]. The other range operated at 100 GHz and had a layout similar to the 240 GHz range. Automated stepper motors were used to accurately control the azimuth and elevation angles of the materials under test. Two images of the brushed concrete sample mounted on a low RCS pylon in the 100 GHz range are shown in Figure 1. Both the HH (horizontal polarization transmit and receive) RCS and the VV (vertical polarization transmit and receive) RCS were measured. Once the RCS of the surfaces were measured, inverse synthetic aperture radar (ISAR) imagery was generated and analyzed to obtain an average backscattering coefficient, σ^0, of the sample, defined here as the RCS per unit illuminated area.

Report Documentation Page

Form Approved
OMB No. 0704-0188

1. REPORT DATE	2. REPORT TYPE	3. DATES COVERED
JUN 2013		**00-00-2013 to 00-00-2013**

4. TITLE AND SUBTITLE	5a. CONTRACT NUMBER
Backscattering of Ground Terrain and Building Materials at Millimeter-Wave and Terahertz Frequencies	5b. GRANT NUMBER
	5c. PROGRAM ELEMENT NUMBER
6. AUTHOR(S)	5d. PROJECT NUMBER
	5e. TASK NUMBER
	5f. WORK UNIT NUMBER
7. PERFORMING ORGANIZATION NAME(S) AND ADDRESS(ES) **University of Massachusetts Lowell,Submillimeter-Wave Technology Laboratory,Lowell,MA,01854**	8. PERFORMING ORGANIZATION REPORT NUMBER
9. SPONSORING/MONITORING AGENCY NAME(S) AND ADDRESS(ES)	10. SPONSOR/MONITOR'S ACRONYM(S)
	11. SPONSOR/MONITOR'S REPORT NUMBER(S)

12. DISTRIBUTION/AVAILABILITY STATEMENT
Approved for public release; distribution unlimited

13. SUPPLEMENTARY NOTES
in Passive and Active Millimeter-Wave Imaging XVI, edited by David A. Wikner, Arttu R. Luukanen, Proceedings of SPIE Vol. 8715, June 2013.

14. ABSTRACT
As terrestrial remote sensing and communication systems continue to evolve in the 0.1 ? 0.3 THz band, the need to understand the scattering behavior of common materials and ground terrain at these frequencies becomes important. Terrain features and surface roughness that would otherwise appear smooth at longer wavelengths begin to significantly impact the radar cross section of the surfaces at these higher frequencies. The HH and VV polarized backscattering coefficient of several types of ground terrain and building materials were measured in indoor compact radar ranges operating at 100 GHz and 240 GHz. Measurements of the various materials were collected at elevation angles ranging from 5 to 35 degrees. The goal of the effort was to develop a better understanding of the polarimetric scattering behavior of materials in the 0.1 ? 0.3 THz region.

15. SUBJECT TERMS

16. SECURITY CLASSIFICATION OF:			17. LIMITATION OF ABSTRACT	18. NUMBER OF PAGES	19a. NAME OF RESPONSIBLE PERSON
a. REPORT **unclassified**	b. ABSTRACT **unclassified**	c. THIS PAGE **unclassified**	**Same as Report (SAR)**	**17**	

Figure 1: Photos of the brushed concrete on a low RCS pylon and tipped to 15 degrees elevation. The concrete is at 0 degrees azimuth on the left and 45 degrees azimuth on the right.

The surface roughness of the concrete and shingle materials was measured by using a stylus profilometer. A 2 micron diameter conical tip stylus scanned the rough surface and provided a height profile. A stylus profilometer could not be used for the sand and soil since the stylus would disturb the surface. Instead, an optical profilometer was used in order to obtain a 3D height profile of the soil and sand. A surface profile of the gravel was unable to be acquired due to the large variations in the gravel's surface height.

1.2. Sample Preparation

All materials, except for the roofing shingles, investigated in this work were held in 18 inch x 18 inch x 1.75 inch acrylic containers. The containers were deep enough to ensure that the transmission through the material was very low and that scattering from the sample mount and pylon could be neglected. The asphalt roofing single was attached to 24 inch x 24 inch x 0.5 inch plywood. Care was taken to ensure that the ISAR analysis of the asphalt roofing shingles did not include transmittance effects due to the asphalt shingles and plywood.

1.2.1 Concrete Preparation

Two concrete slabs were prepared and are shown in Figure 2. A trowel was used to spread the wet concrete in the first container then allowed to cure without any further surface finishing. The second concrete surface was troweled and then brushed with a dry paintbrush to impart a roughened texture to the surface. Both concrete slabs were mixed using Quikrete 5000 concrete mix, which is a concrete mix that is labeled for sidewalk construction use. According to the manufacturer, the compressive strength of the concrete takes three days to achieve half strength and 28 days to reach to full strength. Radar measurements on the concrete occurred between 5 and 30 days following pouring.

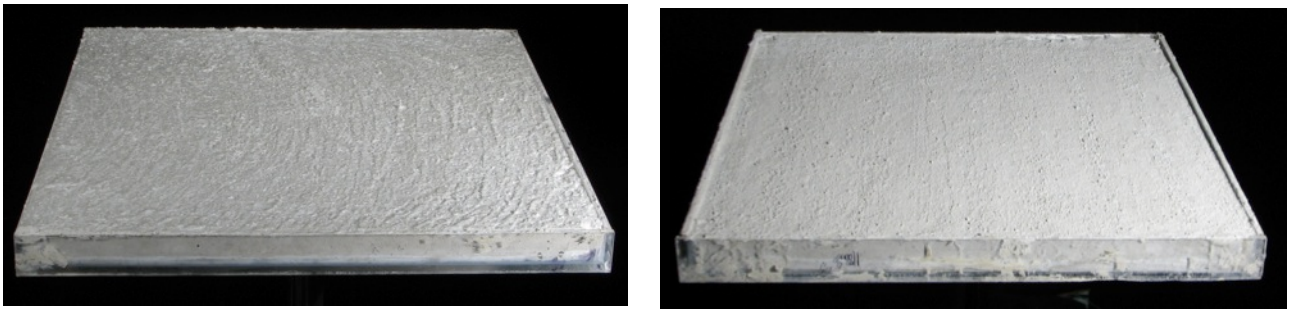

Figure 2: Unbrushed concrete (left) and brushed concrete (right).

1.2.2 Soil Preparation

The soil terrain was made from a purchased bag of generic topsoil that consisted of course organic soil as well as some small twigs and stones. The soil was first baked in a vacuum oven at 120 degrees Celsius for over 24 hours, which removed virtually all of the water from the soil. The soil was then sifted using coarse screens to remove large aggregates. A fine screen with 2.1 mm x 2.1 mm square openings was used to obtain a uniform surface and is shown in Figure 3.

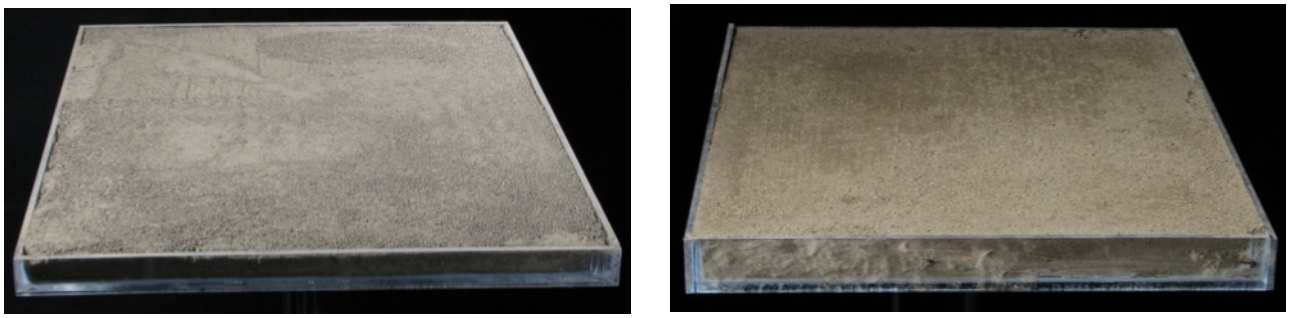

Figure 3: Dry soil (left) and moist soil (right). The moist soil was photographed approximately one hour after water was mixed into the soil.

The soil was placed in the acrylic containers and excess soil was used to determine the volumetric moisture content (VMC). Soil water content was determined by massing the excess soil before and after heating the soil in a 180 degree Celsius oven for four hours. The difference in mass was attributed to the mass of the water in the soil. To determine the volumetric moisture content, the density of the dry soil needed to be determined. Using a graduated cylinder and recording the mass of the soil, a set of density measurements was obtained. The average density, $\rho_{drysoil}$, was measured to be 1.19 g/cm^3. With the dry soil density, the mass of the water in the sample, and the mass of the dry soil, the VMC was determined using Equation (1).

$$VMC = \frac{m_{water}}{m_{drysoil}} \rho_{drysoil}. \quad (1)$$

It must be noted that the VMC of the soil did not remain constant throughout the radar measurements which took approximately 3 to 5 hours for a single 360 degree azimuth sweep at a given elevation angle. Therefore, moisture measurements were taken before the soil was placed in the radar range and immediately after the set of all RCS measurements, which was approximately 12 to 24 hours after measurement initiation. The soil dried out from the top down. Future RCS measurements on moist soil will take advantage of the fact that the RCS of most soil terrain is largely independent of azimuth angle and hence, full 360 degree azimuth sweeps are not required.

In addition to the VMC, the particle size distribution of the soil was estimated. By using fine mesh screens with holes that ranged from 212 microns to 45 microns, a partial particle size distribution of the soil was determined. It was determined that 96% of a sample mass contained particulates that were larger than 45 microns.

1.2.3 Sand Preparation

The sand terrain used was prepared from Quikrete All-Purpose sand and is shown in Figure 4. The density of the sand was measured using the same method as the soil and had a density of 1.68 g/cm^3. The moisture content of the sand was also measured, but there was no difference between the mass of the sand before and after heating.

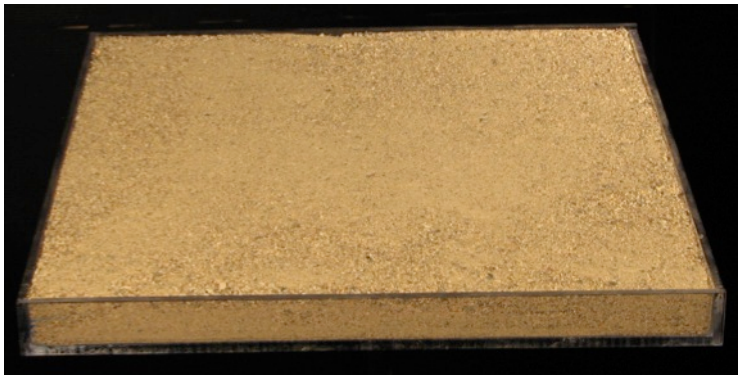

Figure 4: Quikrete All-Purpose sand.

1.2.4 Gravel Preparation

The gravel terrain was prepared from Quikrete All-Purpose gravel and is shown in Figure 5. The average diameter of the aggregates was approximately 10 mm. A visual inspection of the gravel surface was done to ensure that the acrylic container could not be seen through voids between the gravel.

Figure 5: Quikrete All-Purpose gravel.

1.2.5 Asphalt Roofing Shingle Preparation

The asphalt roofing shingle, shown in Figure 6, was attached to a 0.5 inch thick plywood sheet using standard roofing nails. The shingles were laid out so that each row covered half of the shingle material of the row below. The excess shingle material was allowed to overhang the plywood backing on one edge.

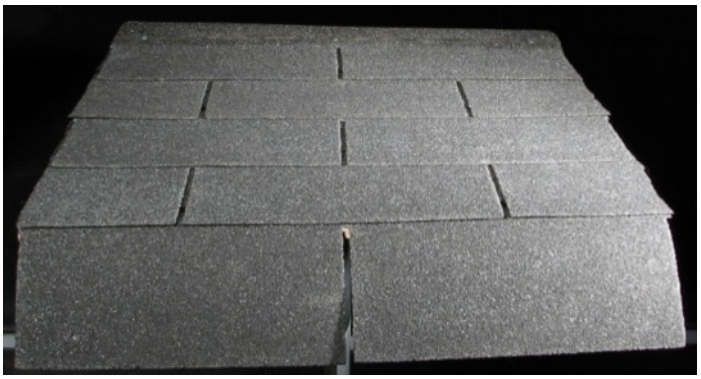

Figure 6: Asphalt roofing shingle shown at 180 degree azimuth.

2. SURFACE ROUGHNESS AND BACKSCATTERING MEASUREMENTS

2.1 Surface Roughness Data

Two main parameters commonly measured when studying the roughness of a surface are the root mean square (rms) roughness, s, and the correlation length, L. The rms roughness is a root mean square average of the heights above or below a mean reference line. The correlation length gives a measure of how far two points must be separated along the mean reference line before their heights are considered uncorrelated. In order to calculate the correlation length, the autocovariance function, C(x), must first be computed using equation (2).

$$C(m*\Delta x) = \frac{1}{s^2}\frac{1}{N-M}\sum_{j=1}^{N-M}(H_j * H_{j+m}); m = 1,2,3,...,M. \quad (2)$$

H_j and H_{j+m} are the measured profile heights at discrete points j and j+m, where j=1 was the first point and j=N was the last point of the height profile. The value of Δx depended on which profilometer was used. For the stylus profilometer, Δx was 5 microns. For the optical profilometer, Δx was 1 micron. The correlation length is then defined as the value where $C(L) = e^{-1} \approx 0.368$. The quantity ks, where k is the free space wavenumber $2\pi c/f$, was calculated to give a quantifiable value to roughness when compared to the frequency. Even though the roughness could not be measured for the gravel, it is assumed that ks was much greater than 1 due to the loose packing and the large size of the gravel rocks. The rms roughness, correlation length, and ks values for the materials in this study are shown in Table I. The correlation lengths measured for the sand and the soil could not be accurately acquired from the optical profilometer and are not reported.

Table I. Roughness parameters and ks values of the samples studied.

Sample	s (microns)	L (microns)	ks at 100 GHz	ks at 240 GHz
Unbrushed Concrete	96	799	0.200	0.481
Brushed Concrete	136	576	0.284	0.683
Soil	190	No Measurement	0.398	0.954
Sand	201	No Measurement	0.422	1.012
Gravel	N/A	N/A	Assumed >1	Assumed >1
Shingles	137	437	0.288	0.690

2.2 ISAR Imagery

A typical ISAR image generated in this work is shown in Figure 7. Each pixel of the ISAR image corresponds to a specific position on the material under test and effectively gives the RCS of the rough surface at that location. By summing the RCS of each pixel in a selected area, the total RCS of that selected area was obtained. The backscatter coefficient σ^0 was obtained by dividing the total RCS by the selected area. By calculating σ^0 over a user selected area, one could ensure that edge scattering or the mounting pylon did not influence the value of σ^0. The value of σ^0 for each material in Table I was measured at multiple azimuthal angles for a given elevation angle. The values of σ^0_{HH} and σ^0_{VV} given in the next section were the average of σ^0 measured at these multiple azimuthal angles. All of the materials studied, except for the asphalt roofing shingles, had a σ^0 that was independent of azimuth angle.

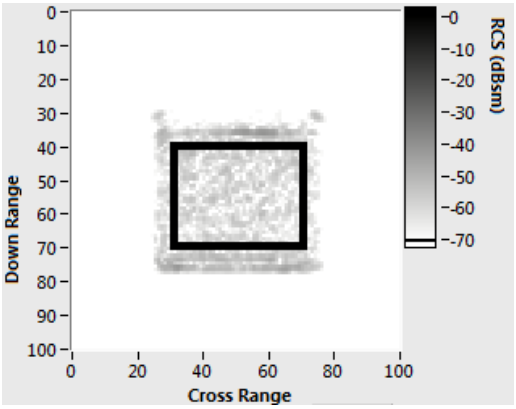

Figure 7: Sample ISAR image of unbrushed concrete at 35 degrees elevation, 0 degree azimuth, and with HH polarization. Only scattering from the boxed section was used to calculate σ^0.

2.3 Backscatter Results

The backscattering coefficient data for all of the materials measured are shown in Figure 9 to Figure 20. The soil measurements proved somewhat challenging because the soil moisture, and therefore its dielectric constant [2], did not remain constant throughout the radar measurement, which can be seen as a change in color of the soil from Figure 8. Due to mounting constraints, obtaining RCS measurements as quickly as possible required that the RCS data be acquired first at 20 degrees elevation and then at 5, 10, and 15 degrees elevation. The soil was then at its "wettest" at 20 degrees and

progressively got drier at 5, 10, and 15 degrees. Moisture measurements of the soil were obtained before the radar measurements began and approximately 12 to 24 hours after water was mixed into the soil. The VMC values are shown in Table II. However, it was observed that the roughness of the soil did not change much as the soil dried.

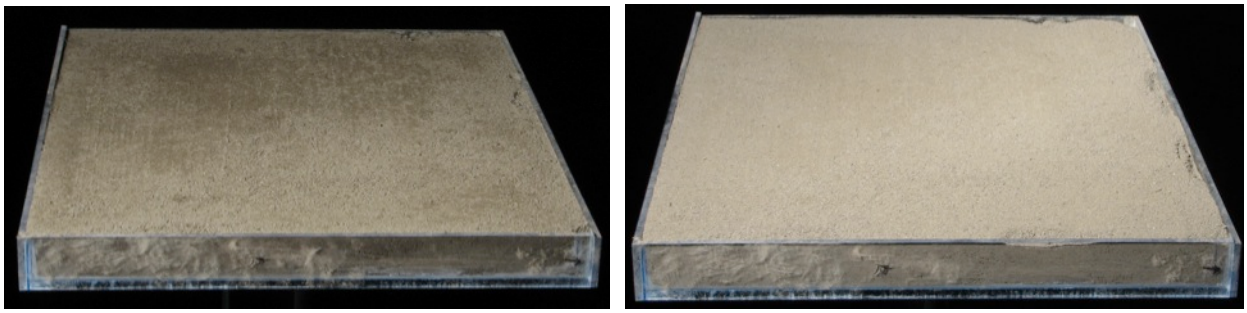

Figure 8: Soil before (left) and after (right) RCS measurement. The color of the soil changes from dark to light as the VMC decreases. Photos taken approximately 12 hours apart.

Table II. Moisture content of soil.

Measurement	**Frequency Measured (GHz)**	**Initial Moisture (g/cm^3)**	**Final Moisture (g/cm^3)**
Dry Soil	100	0.05	No Measurement
Dry Soil	240	0.03	0.10
Moist Soil	100	0.16	0.09
Moist Soil	240	0.23	0.08
Moist Soil	100	0.14	0.05

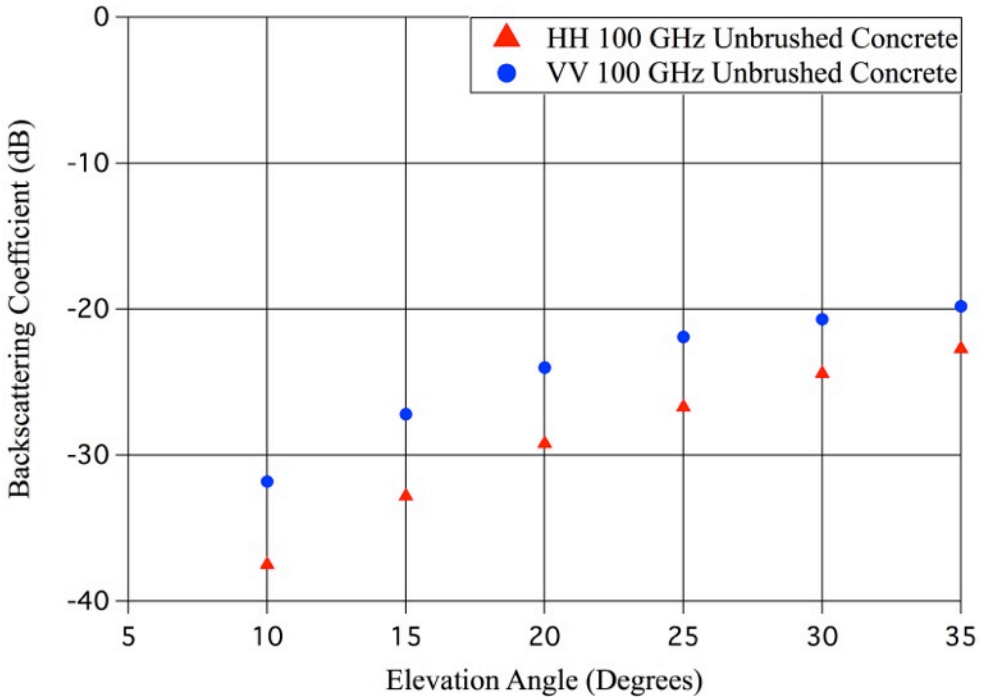

Figure 9: HH and VV polarized backscattering coefficients for unbrushed concrete at 100 GHz.

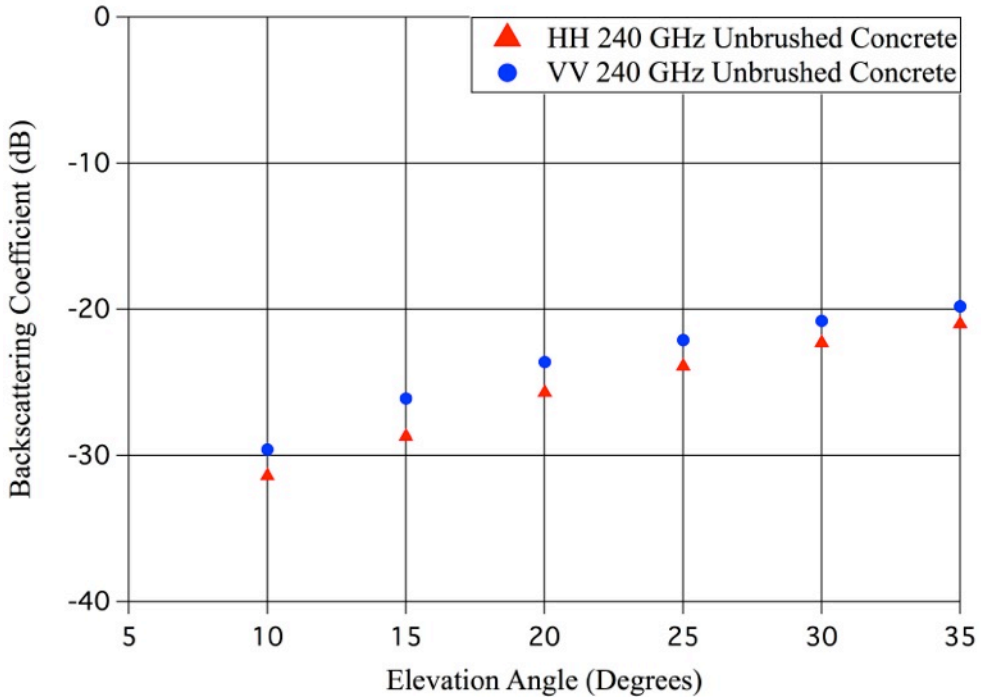

Figure 10: HH and VV polarized backscattering coefficients for unbrushed concrete at 240 GHz.

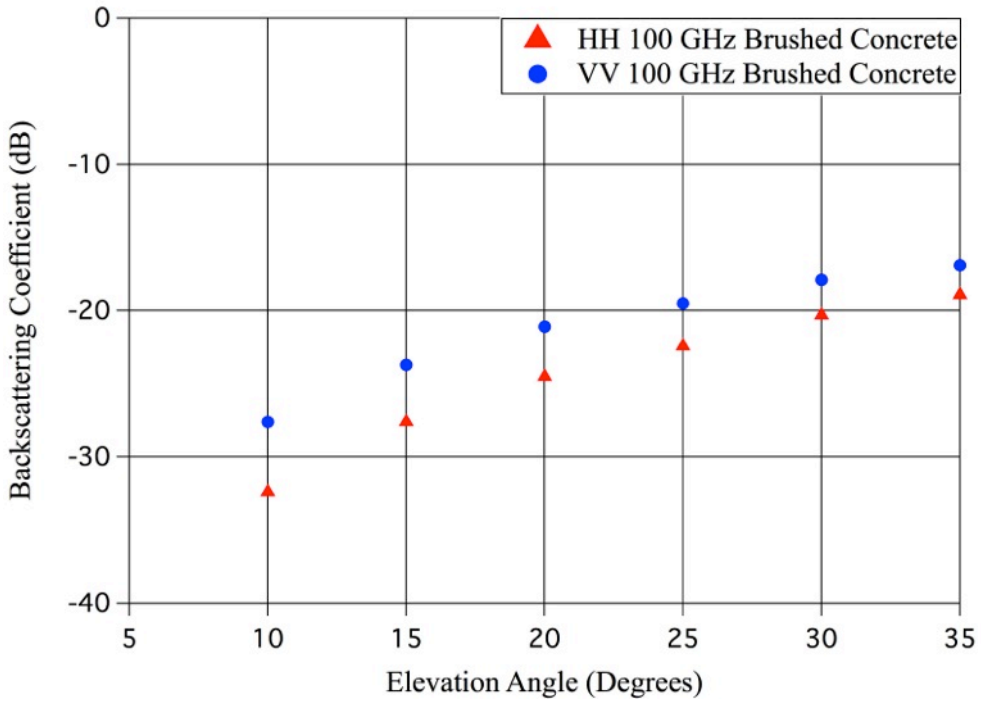

Figure 11: HH and VV polarized backscattering coefficients for brushed concrete at 100 GHz.

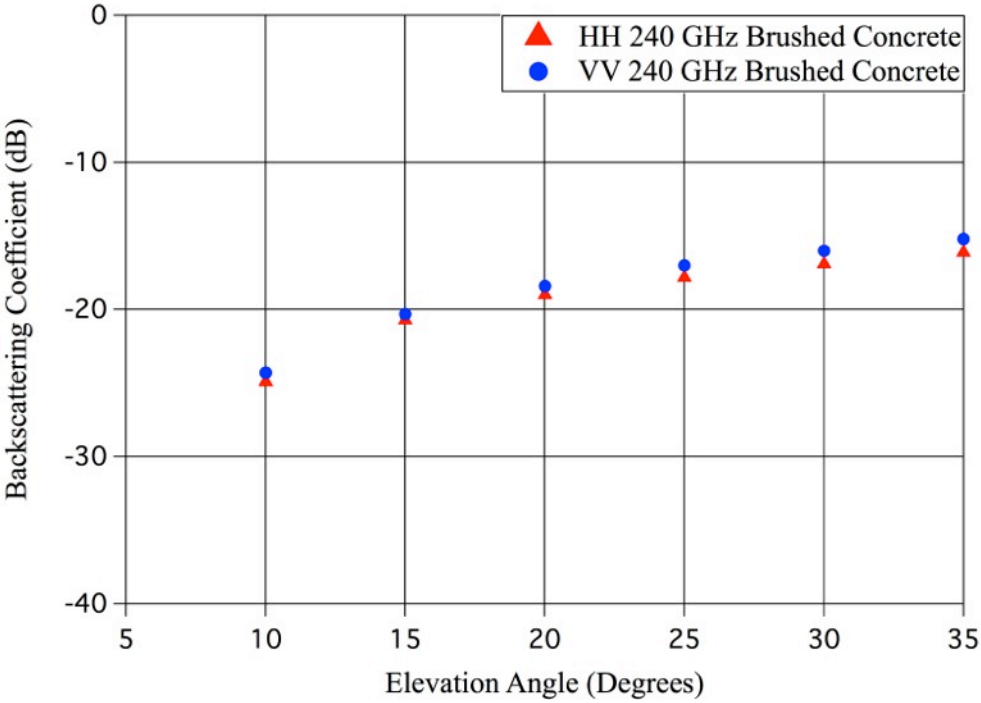

Figure 12: HH and VV polarized backscattering coefficients for brushed concrete at 240 GHz.

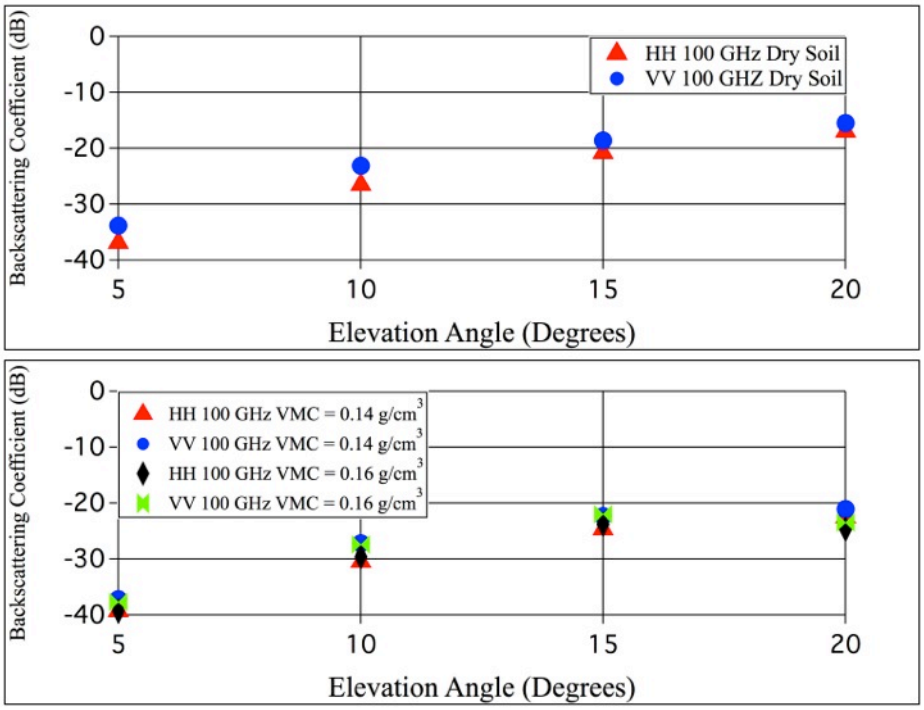

Figure 13: HH and VV polarized backscattering coefficients for dry (top) and moist (bottom) soil at 100 GHz.

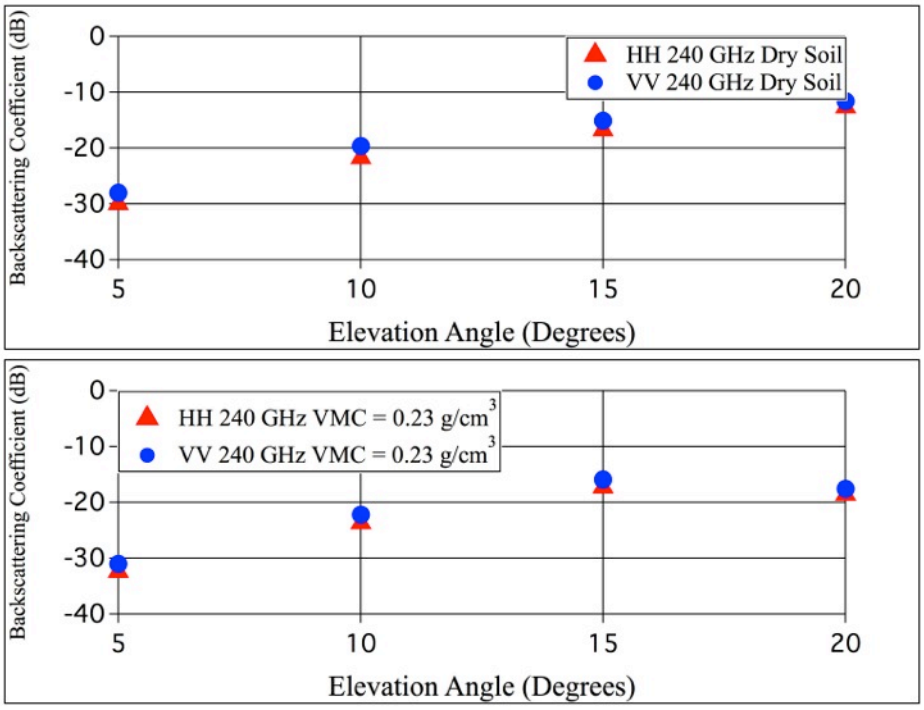

Figure 14: HH and VV polarized backscattering coefficients for dry (top) and moist (bottom) soil at 240 GHz.

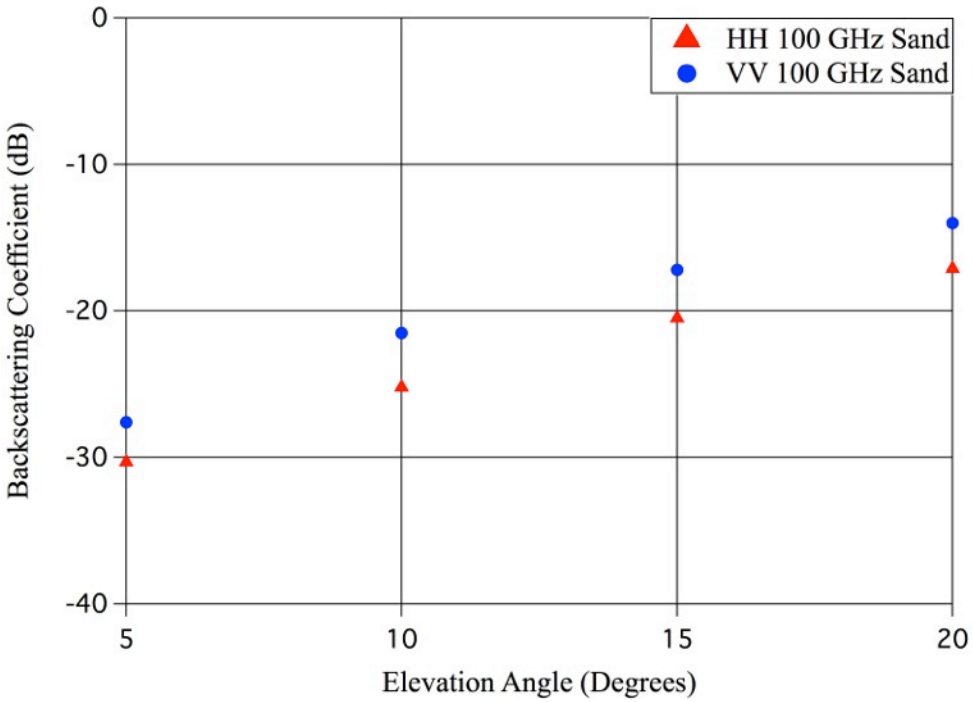

Figure 15: HH and VV polarized backscattering coefficients for sand at 100 GHz.

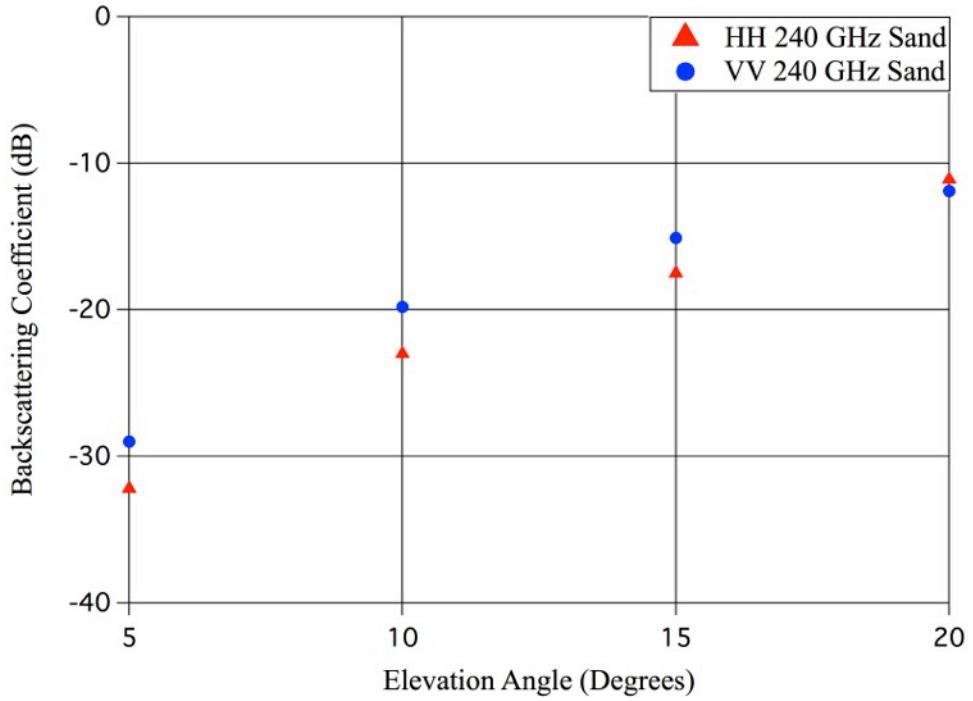

Figure 16: HH and VV polarized backscattering coefficients for sand at 240 GHz.

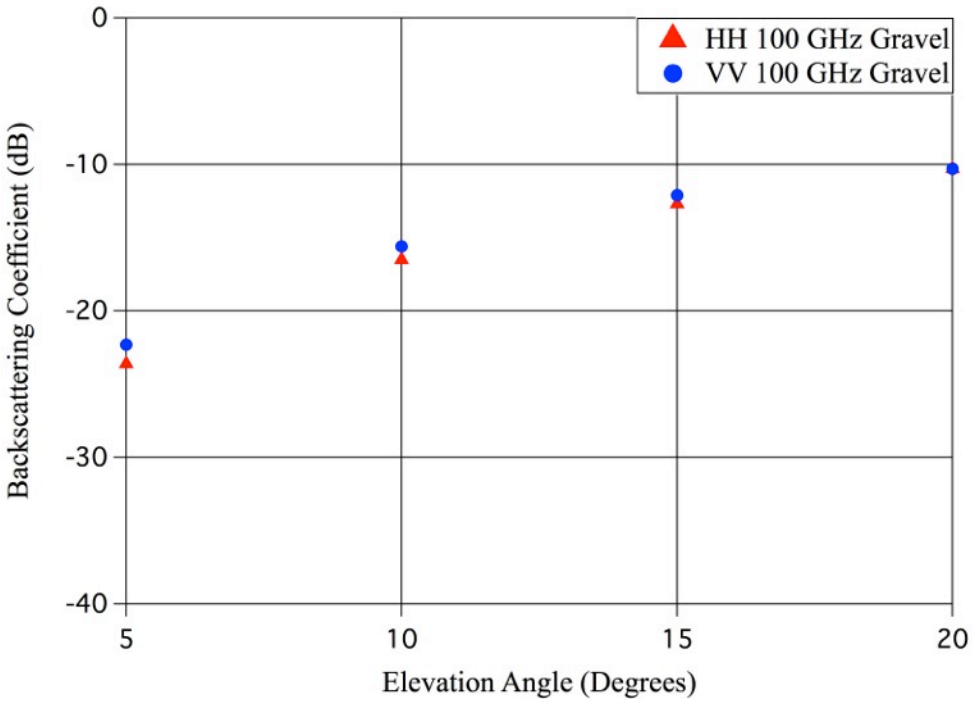

Figure 17: HH and VV polarized backscattering coefficients for gravel at 100 GHz.

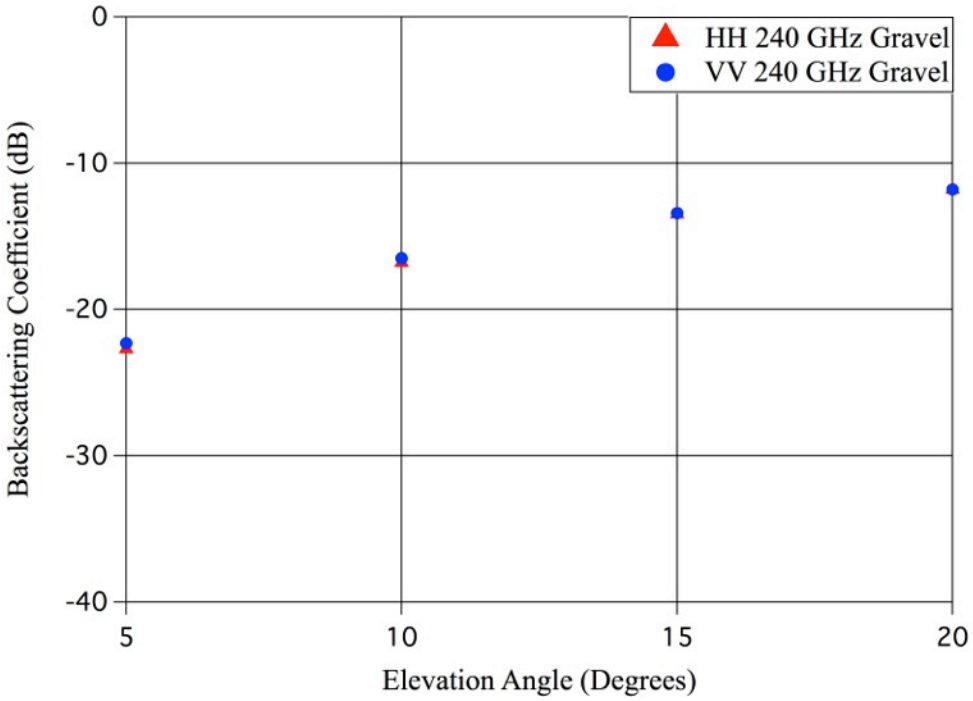

Figure 18: HH and VV polarized backscattering coefficients for gravel at 240 GHz

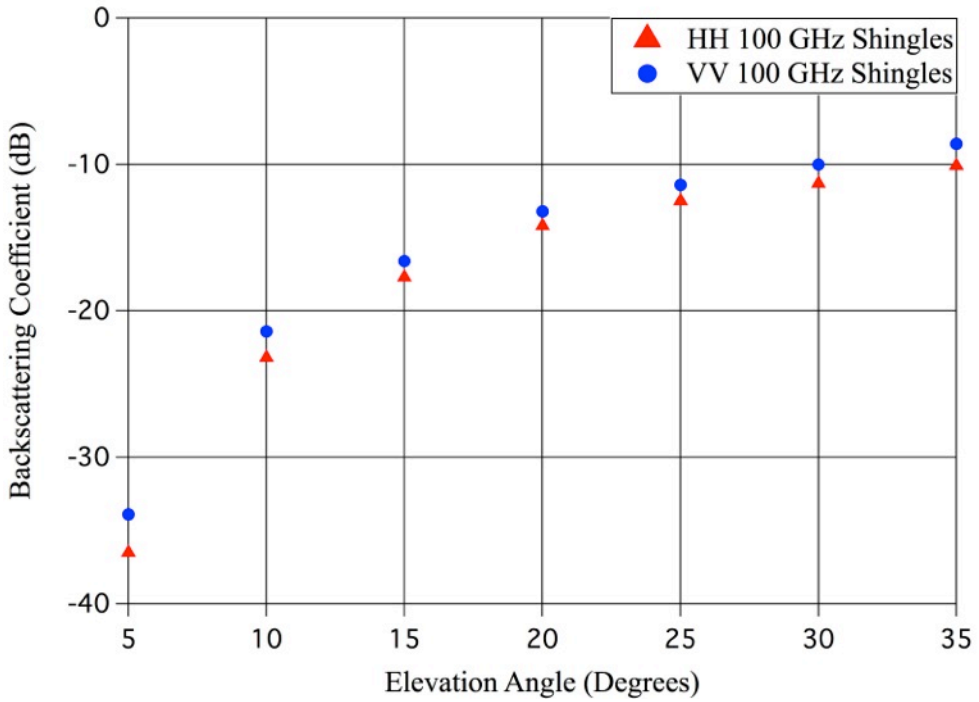

Figure 19: HH and VV polarized backscattering coefficients for shingles at 100 GHz.

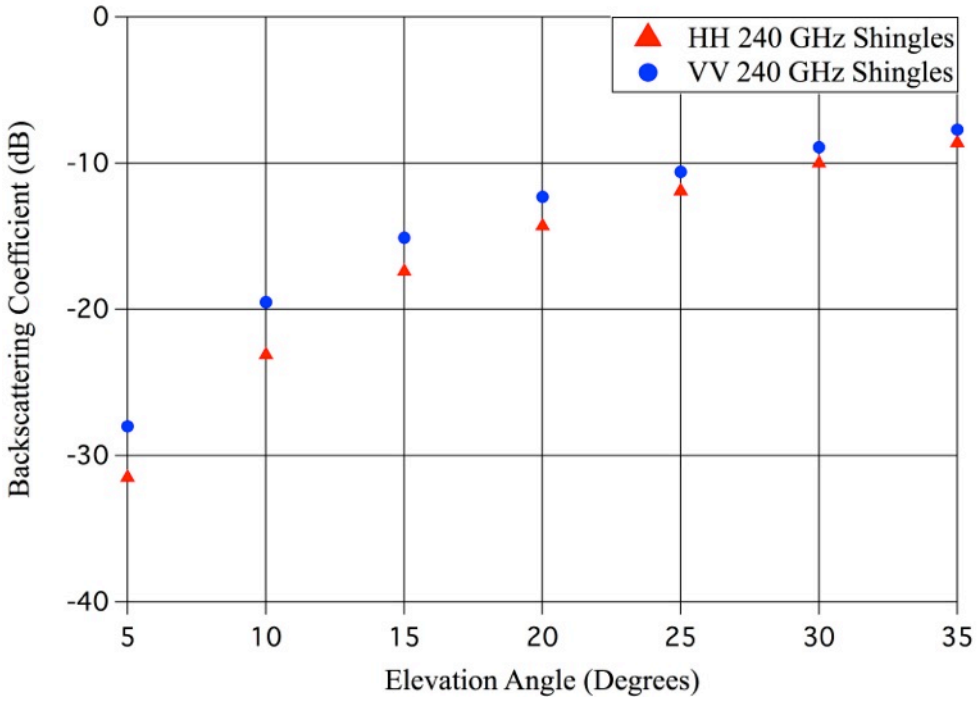

Figure 20: HH and VV polarized backscattering coefficients for shingles at 240 GHz.

3. DISCUSSION

3.1 Concrete Analysis

The value of σ^0 as a function of the roughness parameter ks was investigated for the two concrete slabs. As the value of ks increased, the copolarization ratio, $\sigma^0_{HH}/\sigma^0_{VV}$ (calculated in linear space), approached 1, as shown in Figure 21. The trend where $\sigma^0_{HH}/\sigma^0_{VV}$ approaches unity as ks increases is well-known and has been observed by others at microwave, millimeter-wave, and THz frequencies [3], [4], and [5]. Due to radar system limitations, the σ^0 value for both concrete slabs at 5 degrees elevation was unable to be acquired.

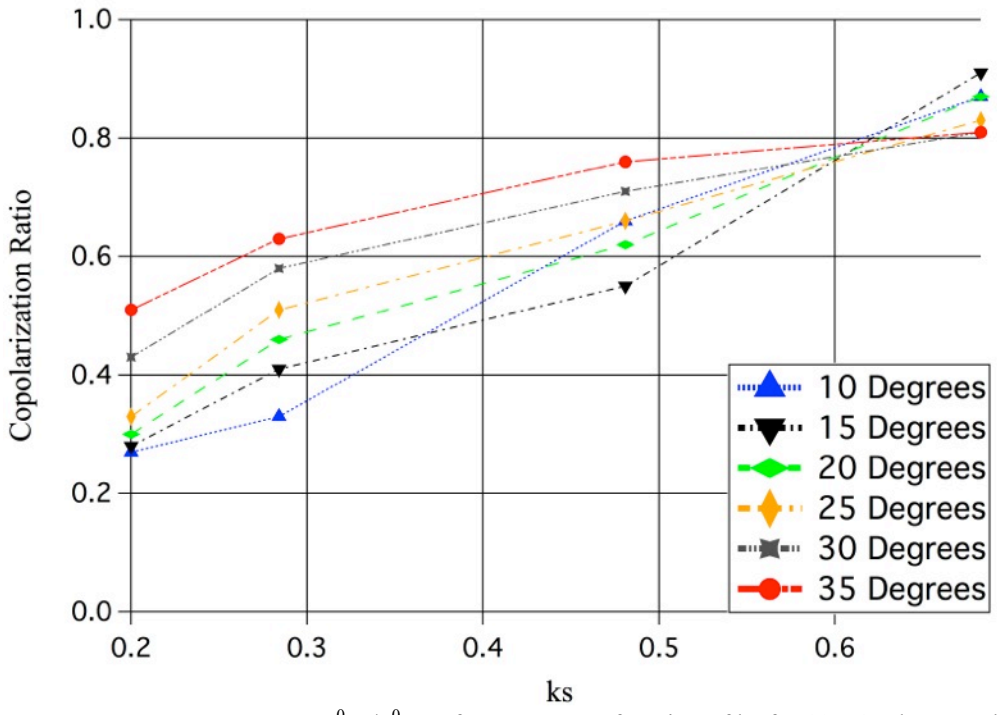

Figure 21: The copolarization ratio, $\sigma^0_{HH}/\sigma^0_{VV}$, of concrete as a function of ks for 10 – 35 degrees elevation.

3.2.1 Soil Analysis

The change in moisture content needed to be taken into account when analyzing the values of σ^0 for the soil surfaces. For the dry soil measurements, the moisture content increased from 0.03 g/cm^3 to 0.10 g/cm^3 as the radar measurements progressed and led to an increase in the soil's dielectric constant. For the moist soil measurements, the moisture content decreased, from approximately 0.18 g/cm^3 to 0.07 g/cm^3. Even though the dielectric properties of the soil were changing throughout the radar measurement, according to reference [6], the value of σ^0 has a much stronger dependence on the terrain's roughness parameters compared to the terrain's dielectric constant. Again, we noted that the soil roughness did not change much as the soil dried.

The measured value of σ^0 for the moist soil was lower compared to the dry soil for all elevation angles and frequencies. It was also seen that σ^0 decreased for the three moist soil RCS measurements when the elevation angle went from 15 degrees, which was taken near the end of the RCS measurement set, to 20 degrees, which was taken when the soil was at its highest VMC value. If surface scattering was the only factor, then it is expected that σ^0 would increase when moisture is added and the dielectric constant increases. However, the opposite behavior was observed in the data. One possible explanation for this observation could be that a change in the volumetric scattering properties of the terrain occurred as the material transitions from moist soil to dry soil. Dry and moist soil radar scattering measurements performed by Nashashibi [7] showed that σ^0 was lower for moist soil than for dry soil at 94 GHz (but not at 35 GHz). Nashashibi explains that volumetric scattering effects due to the air voids in the soil become significant for dry soil as the frequency approaches the millimeter-wave and terahertz regime. The volumetric scattering effect decreases as the soil moisture increases because of the increase in the attenuation of the moist soil.

3.2.2 Sand Analysis

The σ^0 of sand was within 2 dB of σ^0 for dry soil for elevation angles of 10 degrees and higher. This similarity can be explained by the similar roughness (s_{sand} = 201 microns and s_{soil} = 190 microns) of the sand and dry soil samples. In addition, the dielectric constant of dry soil is expected to be very similar to dry sand at these frequencies since both samples had similar moisture contents.

3.2.3 Gravel Analysis

The copolarization ratio for gravel is shown below in Table III for 100 GHz and 240 GHz. Even though the rms roughness could not be measured for the gravel, ks was certainly larger at 240 GHz than at 100 GHz. The data shown in Table III is consistent with the trend that the copolarization ratio approaches 1 as ks increases.

Table III. Copolarization ratio of gravel at 100 GHz and 240 GHz.

Elevation angle (degrees)	**$\sigma^0_{HH}/\sigma^0_{VV}$ at 100 GHz**	**$\sigma^0_{HH}/\sigma^0_{VV}$ at 240 GHz**
5	0.74	0.91
10	0.81	0.93
15	0.87	0.98
20	1.00	1.00

3.2.4 Asphalt Roofing Shingle Analysis

Unlike the other materials studied, the organized pattern of the shingled surface caused σ^0 to have an azimuthal dependence. Steps where shingles overlapped caused larger RCS returns, as shown in Figure 22 (right). The larger returns were observed for both HH and VV polarizations. These large returns were only observed for low elevation angles. As the elevation angle increased, shingle edge scattering somewhat blended in with the increasing RCS from the rest of the shingle, as shown in Figure 23.

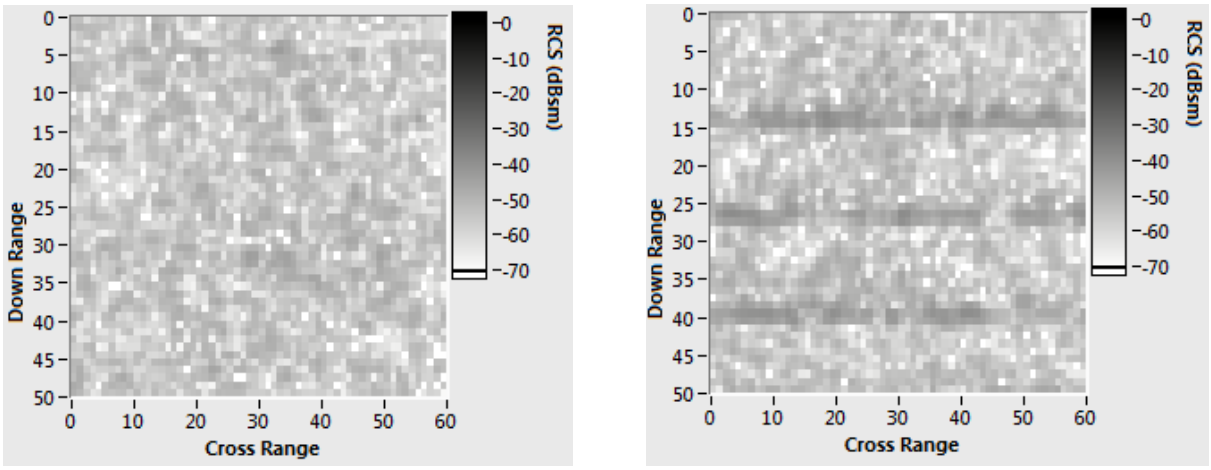

Figure 22: ISAR imagery of the asphalt roofing shingle at 15 degrees elevation and 100 GHz. The left image is at an azimuth of 0 degrees and σ^0 was measured to be -18.9 dB. The right image is at an azimuth of 180 degrees and σ^0 was measured to be -13.7 dB.

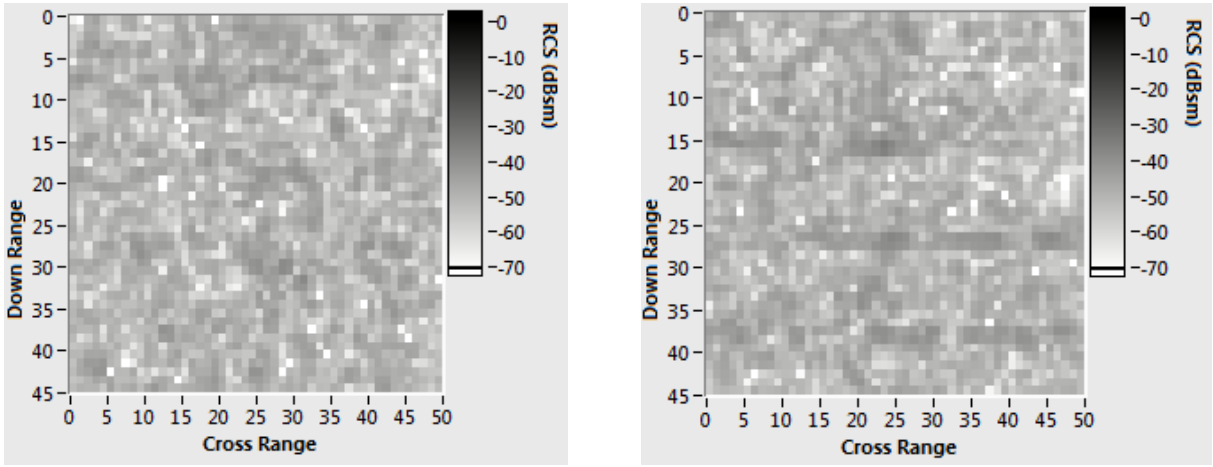

Figure 23: ISAR imagery of the asphalt roofing shingle at 35 degrees elevation and 100 GHz. The left image is at an azimuth of 0 degrees and σ^0 was measured to be -10.4 dB. The right image is at an azimuth of 180 degrees and σ^0 was measured to be -10.0 dB.

4. CONCLUSION

The millimeter-wave and terahertz backscattering properties of various ground terrain and building materials were investigated at low elevation angles. Similar to what is observed in the microwave region, the backscattering coefficient increased as the elevation angle increased for virtually all the materials studied. In addition to elevation angle, the value of σ^0 was, on average, approximately 2 dB higher for the materials measured at 240 GHz compared to 100 GHz. For surfaces, such as gravel and the two concrete slabs, the ratio between σ^0_{HH} and σ^0_{VV} approached unity as ks increased. Future measurements will focus on exercising more control on soil moisture content to better understand the impact of both moisture and roughness on soil backscattering at these frequencies.

5. REFERENCES

[1] DeMartinis, G. B., Coulombe, M. J., Horgan, T. M., Giles, R. H., Nixon, W. E., "A 240 GHz Polarimetric Compact Range for Scale Model RCS Measurements," Antenna Measurements Techniques Association, 3-8 (October 2010)

[2] Ulaby, F. T., Moore, R. K., Fung, A. K., [Microwave Remote Sensing Active and Passive, Volume III], Artech House, Norwood MA, (1986)

[3] Long, M. W., [Radar Reflectivity of Land and Sea], D.C. Heath and Company, Lexington MA, (1975)

[4] Ulaby, F. T., Nashashibi, A., El-Rouby, A., Li, E. S., De Roo, R. D., Sarabandi, K., Wellman, R. J., Wallace, H. B., "95-GHz Scattering by Terrain at Near-Grazing Incidence," IEEE Transactions on Antennas and Propagation 46(1), 3-13 (January 1998)

[5] Gatesman, A. J., Goyette, T. M., Dickinson, J. C., Giles, R. H., Waldman, J., Sizemore, J., Chase, R. M., Nixon, W. E., "Polarimetric backscattering behavior of ground clutter at X, Ka, and W-band," Proc. SPIE 5808, 428-439 (2005)

[6] Ruck, G. T., Barrick, D.E., Stuart W. D., Krichbaum C. K., [Radar Cross Section Handbook, Volume 2], Plenum Press, New York & London, (1970)

[7] Nashashibi, A., Ulaby, F. T., Sarabandi, K., "Measurement and modeling of the millimeter-wave backscatter response of soil surfaces," IEEE Transactions on Geoscience and Remote Sensing 34(2), 561-572 (March 1996)